

Signal-Aligned Network Coding for Multicell Processing With Limited Cooperation

Tse-Tin Chan¹, *Student Member, IEEE*, and Tat-Ming Lok¹, *Senior Member, IEEE*

Abstract—This paper puts forth an interference mitigation scheme, named signal-aligned network coding (SNC), for both uplink and downlink cloud radio access networks (C-RANs). The base stations (BSs) are connected to a central processor (CP) via digital links with individual limited capacities. The user equipments (UEs) communicate with the CP through BSs serving as relay nodes. We focus on the situation that the digital links have moderate rate constraint. Loosely speaking, the capacities of the digital links and the wireless links are of the same order of magnitude. The SNC scheme strategically aligns the signals by signal alignment (SA) and then decodes the aligned signals by physical-layer network coding (PNC). With the proper designs of the network-coded messages transmitted and the alignment of signals, the SNC scheme significantly mitigates the inter-cell interference. No matter the size of the network, the SNC scheme achieves full degrees of freedom (DoF) asymptotically. For the finite signal-to-noise ratio (SNR) performances, simulation results show that the SNC scheme achieves superior sum-rate than the conventional compute-and-forward scheme in the two-user and the three-user cases, especially in the high SNR regime.

Index Terms—Cloud radio access network (C-RAN), degrees of freedom (DoF), distributed MIMO, interference alignment (IA), physical-layer network coding (PNC).

I. INTRODUCTION

WITH the rapid growth of mobile data traffic, cellular systems are moving towards denser cell deployment. Inter-cell interference becomes a crucial problem in future networks [3]. Cloud radio access network (C-RAN) is a promising network architecture to manage inter-cell interference by enabling multicell processing via wired links [4]. In the C-RAN architecture, base stations (BSs) are connected to a central processor (CP) through the wired links. A significant hindrance to the C-RAN is the rate constraint on the wired links [5].

In this paper, we put forth the signal-aligned network coding (SNC) scheme for both uplink and downlink K -user

Manuscript received October 10, 2019; revised February 24, 2020 and April 21, 2020; accepted April 29, 2020. Date of publication May 6, 2020; date of current version August 14, 2020. This work was supported by the General Research Fund from the Research Grants Council, Hong Kong, under Project CUHK 14203616. This article was presented in part at the IEEE/CIC International Conference on Communications in China, 2018 and in part at the IEEE International Conference on Signal Processing, Communications and Computing, 2018. The associate editor coordinating the review of this article and approving it for publication was L. Ong. (*Corresponding author: Tse-Tin Chan.*)

The authors are with the Department of Information Engineering, The Chinese University of Hong Kong, Hong Kong (e-mail: ctt014@ie.cuhk.edu.hk; tmlok@ie.cuhk.edu.hk).

Color versions of one or more of the figures in this article are available online at <http://ieeexplore.ieee.org>.

Digital Object Identifier 10.1109/TCOMM.2020.2992719

0090-6778 © 2020 IEEE. Personal use is permitted, but republication/redistribution requires IEEE permission. See <https://www.ieee.org/publications/rights/index.html> for more information.

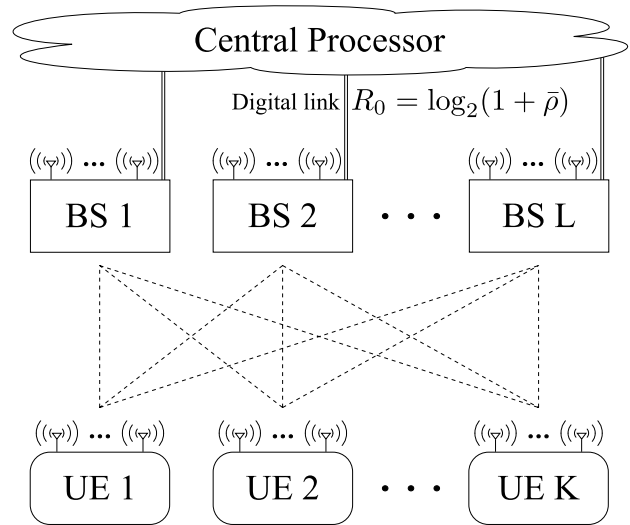


Fig. 1. A MIMO C-RAN consisting of K user equipments (UEs), L base stations (BSs), and a central processor (CP).

equipment (UE) L -BS time-varying MIMO C-RANs as shown in Fig. 1. The BSs are connected to the CP via the independent digital links with restricted rates. We focus on adopting digital links with moderate individual rate constraints. Loosely speaking, the rate constraints on the digital links and the capacities of the wireless links are of the same order of magnitude. Transmitting analog signals of the messages or the raw analog signal samples via the wired links is not possible owing to the excessive data rate required. Therefore, joint decoding (uplink) or joint precoding (downlink) of the raw signals directly is not possible. Advanced schemes for handling the inter-cell interference are desired.

A. Literature Review

Physical-layer network coding (PNC) [6] brings the promising idea of network coding [7], [8] from the network layer to the physical layer to ease the interference problem in wireless channels. PNC treats interfering signals as a form of network coding and demodulates superimposed signals into network-coded data. Reference [9] presented a design guideline of industrial applicable PNC. It considered a binary system and adopted quadrature amplitude modulation (QAM) schemes. There are many approaches making use of the wireless interference for network coding such as compress-and-forward schemes [10]–[17] and compute-and-forward schemes [18]–[28].

In compress-and-forward schemes, signals are quantized or compressed for allowing joint processing at the CP with the aid of the wired links [10]–[17]. Nevertheless, quantization noise is a significant factor in deteriorating the performance of compress-and-forward schemes. Moreover, some compress-and-forward schemes have high complexities even with a moderate number of total antennas, which make the schemes hard to be implemented.

Compute-and-forward schemes directly generate network-coded messages, which are noiseless linear combinations of the messages over a finite field, from the superimposed interfering signals and utilize them to improve the transmission rate [18]–[28]. The network coding coefficients, which are the coefficients in the combinations of the messages over a finite field, are related to the corresponding channel coefficients. However, two main problems are impairing the performance of compute-and-forward schemes [19], [22]. First, the rank deficiency occurs when the linear combinations of the messages in a finite field are linearly dependent. The rank deficiency causes the messages to be irrecoverable. Second, there is the rate penalty coming from the non-integer parts of the channel coefficients. During decoding, the received signal is scaled to make the effective channel coefficients closer to the desired integer coefficients. The remaining non-integer part would be treated as noise. This scaling factor also results in amplification of the received noise. In general, none of compress-and-forward schemes and compute-and-forward schemes outperforms others in all regimes.

References [29], [30] focused on utilizing the advantages of signal alignment (SA), a variation of interference alignment (IA) [31]–[33] to mitigate interference in two-hop interference channels. The relays apply linear transformations to the analog signals so that the interfering analog signals are neutralized at the destinations. However, these schemes cannot be adopted for the model considered in this paper. The main reason is that only digital messages, rather than the raw analog signal samples, can be forwarded via the digital links owing to the rate constraints on the digital links.

Furthermore, we can treat our channel model as a cache-aided C-RAN or fog radio access network (F-RAN) with zero cache size [34], [35]. As far as we concerned, there are two types of approaches introduced in the related literature, namely hard-transfer fronthauling and soft-transfer fronthauling. Nevertheless, our work is different from both types of approaches. Hard-transfer fronthauling means that the fronthaul is used to send the individual messages of all users to every BS in raw form. However, hard-transfer fronthauling requires that the rate-constraint on the fronthaul links is of a much higher order than the capacities of the wireless links. In contrast to hard-transfer fronthauling, our work only requires that the rate-constraint of the digital links and the capacities of the wireless links are of the same order of magnitude. This is because the CP in the SNC scheme only needs to transmit the integer combinations of the messages over the same finite field, rather than the messages of all users in raw form, to each BS. Soft-transfer fronthauling is another approach introduced in the cache-aided C-RAN or F-RAN

literature. Adopting soft-transfer fronthauling, the CP performs zero-forcing beamforming and quantizes the resulting encoded signals. This approach is also introduced in the previous paragraph, called compress-and-forward. Nevertheless, some compress-and-forward schemes have high complexities which makes the schemes hard to be implemented, especially when the number of users is large. In contrast with soft-transfer fronthauling, we are adopting the framework of compute-and-forward for conveying linear combinations of the messages over a finite field between the CP and the BSs utilizing the nested lattice code.

B. Main Contributions

Some researches such as [36]–[42] showed that PNC could be employed together with SA to achieve better performance in different channel models. In this paper, we put forth the SNC scheme which couples PNC and SA in C-RANs with rate-constrained digital links. With the proper designs of the alignment of signals and the network-coded messages decoded, the SNC scheme significantly mitigates the inter-cell interference. Regarding the PNC demodulation, as we focus on the information-theoretic rates of the SNC scheme in this paper, we adopt the fundamental framework of compute-and-forward described in [19] in which superimposed signals are decoded into an integer combination of the codewords utilizing the nested lattice code.

As mentioned in the previous subsection, conventional compute-and-forward schemes have the rank deficiency and non-integer penalty problems [19], [22]. Reference [22] presented a solution to solve the rank deficiency problem. Only a subset of the receivers is activated to keep the linear combinations of the messages decoded in a finite field linearly independent. This idea is promising in the system with plenty of receivers.

In this paper, we utilize PNC and SA to solve the rank deficiency and non-integer penalty problems. Our SNC scheme aligns the transmitted signals at the receivers through precoding so that the network-coded messages obtained at the receivers are linearly independent. As a result, the rank deficiency problem can be solved. Moreover, the effective channels of the signals are aligned in an integer ratio. Hence, the non-integer penalty is also prevented.

References [26]–[28] also consider using PNC and SA in the channel models similar to ours. However, there are significant differences between their works and ours. Our SNC scheme achieves higher degrees of freedom (DoF) than the schemes proposed in [26]–[28], especially when the number of users is large. We show that the SNC scheme asymptotically achieves full DoF in C-RAN with limited cooperation. In other words, at high signal-to-noise ratio (SNR), the SNC scheme achieves approximately the capacity of the channel as if there is unlimited cooperation among the BSs. This asymptotic full DoF achievement is not limited by the number of antennas of each node. This result acts as a benchmark for future studies about coupling PNC and SA. Moreover, simulation results show that the SNC scheme with small numbers of symbol extension achieves better sum-rate than the conventional

compute-and-forward scheme in the finite SNR regime of the two-user and three-user cases.

Furthermore, the alignment matrix, which is also called the network-coded generator matrix in [26]–[28], determines how signals should be aligned. References [26], [27] proposed the alignment matrices for the two and three users cases with specific numbers of antennas at each node. Reference [28] proposed a brute-force method to search for the alignment matrices in general cases, and it causes a high computational complexity. Different from [26]–[28], our paper proposed a general approach to design the alignment matrices for arbitrary numbers of transmitters, receivers, and antennas of each node. The design of the alignment matrices proposed in this paper contributes to the theoretical analysis of PNC and SA.

C. Outline and Notations

The rest of this paper is organized as follows. Section II describes the system model, the performance metrics, and the symbol extension. Section III gives a simple example to show the main idea of the SNC scheme. Section IV presents the details of the SNC scheme. Section V shows the numerical results to evaluate the SNC scheme and compare it with the conventional compute-and-forward scheme. Section VI concludes this paper. The details of various results are given in Appendices A–C.

In this paper, letters of bold upper case, bold lower case, and lower case indicate matrices, vectors, and scalars respectively. $\mathbb{C}^{m \times n}$ is the set of all complex-valued $m \times n$ matrices. $\mathbb{F}_q^{m \times n}$ represents the set of all $m \times n$ matrices in a finite field of size q . \oplus and \otimes are the addition operation and multiplication operation, respectively, over that finite field. \mathbb{Z} is the set of all non-negative integers and \mathbb{Z}^+ is the set of all positive integers. \mathbf{I}_d indicates the $d \times d$ identity matrix. $\text{diag}[\cdot]$ represents a square diagonal matrix with the elements described inside the bracket. Moreover, $(\cdot)^T$, $(\cdot)^H$, $\|\cdot\|$, $|\cdot|$, $\lceil \cdot \rceil$, and $\mathbb{E}[\cdot]$ are transpose, conjugate transpose, Euclidean norm, absolute value, ceiling function, and statistical expectation respectively.

II. PRELIMINARIES

A. System Model

We consider both uplink and downlink time-varying MIMO C-RANs consisting of K UEs, L BSs, and a CP as shown in Fig. 1. We assign unique indices $k \in \{1, 2, \dots, K\}$ and $l \in \{1, 2, \dots, L\}$ to each UE and BS respectively. BS l is connected to the CP via an independent noiseless digital link with a per-link rate constraint. The SNC scheme can also be applied to the model with a total rate constraint on the digital links. We first consider each UE and BS has one antenna, and the multiple antennas cases are investigated later in this paper.

For the uplink, UEs convey messages to the CP with the aid of the BSs serving as relay nodes. Similarly, for the downlink, the CP conveys messages to UEs with the aid of the BSs. We assume that the UEs (uplink) or the BSs (downlink) transmit signals synchronously and share the same time, frequency, and code resources. Furthermore, we assume that instantaneous global channel state information (CSI) is available to

show the significant theoretical DoF gains by the SNC scheme compared with the conventional schemes.

The overall transmission consists of two phases, namely the communications between the UEs and the BSs (UE-BS links) and that between the BSs and the CP (BS-CP links).

1) *UE-BS Links*: In the uplink, the channel output at BS l is

$$y_l^{(u)} = \sum_{k=1}^K h_{l,k}^{(u)} \bar{x}_k^{(u)} + n_l^{(u)} \quad (1)$$

where $\bar{x}_k^{(u)}$ is the input signal of UE k , $h_{l,k}^{(u)}$ is the CSI of the link from UE k to BS l , and $n_l^{(u)}$ is the additive white Gaussian noise (AWGN) term at BS l . The superscript “(u)” indicates the uplink channel. Similarly, in the downlink, the channel output at UE k is

$$y_k^{(d)} = \sum_{l=1}^L h_{k,l}^{(d)} \bar{x}_l^{(d)} + n_k^{(d)} \quad (2)$$

where $\bar{x}_l^{(d)}$ is the input signal of BS l , $h_{k,l}^{(d)}$ is the CSI of the link from BS l to UE k , and $n_k^{(d)}$ is the AWGN term at UE k . The superscript “(d)” indicates the downlink channel. For both the uplink and the downlink, we assume all channel coefficients are independent and identically distributed (i.i.d.) zero-mean unit-variance complex Gaussian random variables. We also assume all noise terms are i.i.d. zero-mean complex Gaussian random variables with variance $(\sigma_l^{(u)})^2$ (uplink) or $(\sigma_l^{(d)})^2$ (downlink). Moreover, the transmit power constraints in the UE-BS links are

$$0 \leq p_k^{(u)} = |\bar{x}_k^{(u)}|^2 \leq p_{k,\max}^{(u)} \quad \text{and} \quad (3)$$

$$0 \leq p_l^{(d)} = |\bar{x}_l^{(d)}|^2 \leq p_{l,\max}^{(d)}. \quad (4)$$

$p_k^{(u)}$ (uplink) and $p_l^{(d)}$ (downlink) are the actual transmit powers for transmitting signals $\bar{x}_k^{(u)}$ (uplink) and $\bar{x}_l^{(d)}$ (downlink) respectively. $p_{k,\max}^{(u)}$ (uplink) and $p_{l,\max}^{(d)}$ (downlink) are the corresponding maximum transmit powers.

2) *BS-CP Links*: In the uplink, BS l forwards messages to the CP through an independent noiseless digital link with a rate constraint $R_0 = \log_2(1 + \bar{\rho})$ where $\bar{\rho}$ denotes the average SNR of the UE-BS links. Similarly, in the downlink, the CP conveys messages to BS l through an independent noiseless digital link with a restricted rate R_0 .

B. Performance Metrics

In this paper, the objective is to investigate how to achieve a higher information rate and theoretical DoF than the conventional schemes for both uplink and downlink C-RANs with limited cooperation presented in Section II-A.

1) *Achievable Information Rate*: The information rates of the users’ messages at SNR ρ are denoted by $R_k(\rho)$, $k \in \{1, 2, \dots, K\}$. The information rate tuple $(R_1(\rho), R_2(\rho), \dots, R_K(\rho))$ is achievable if the error probability of the transmission $P_e \leq \epsilon$ for any $\epsilon > 0$ as the block length goes to infinity.

2) *Achievable Degrees of Freedom (DoF)*: DoF, also known as capacity pre-log or multiplexing gain, provides a first-order approximation to the capacity. Therefore, DoF plays an important role in characterizing the capacity behavior in the high SNR regime. The achievable DoF tuple (d_1, d_2, \dots, d_K) can be derived from the achievable rate tuple $(R_1(\rho), R_2(\rho), \dots, R_K(\rho))$ that

$$d_k = \lim_{\rho \rightarrow \infty} \frac{R_k(\rho)}{\log_2(\rho)}, \quad \forall k \in \{1, 2, \dots, K\}. \quad (5)$$

The total achievable DoF can be found by

$$d_{\text{sum}} = \sum_{k=1}^K d_k. \quad (6)$$

C. Symbol Extension

In the SNC scheme, the system adopts an N symbol extension of the channel where $N \in \mathbb{Z}^+$. A supersymbol collectively denotes the N symbols transmitted from each UE (uplink) or each BS (downlink) over N slots.

1) *UE-BS Links*: In the uplink, UE k modulates i.i.d. message vector $\mathbf{b}_k^{(u)} \in \mathbb{F}_q^{N \times 1}$ to signal vector $\mathbf{x}_k^{(u)} \in \mathbb{C}^{N \times 1}$ over an N symbol extension where

$$\mathbf{b}_k^{(u)} = [b_k^{(u)}(1) \quad b_k^{(u)}(2) \quad \dots \quad b_k^{(u)}(N)]^T, \quad (7)$$

$$\mathbf{x}_k^{(u)} = [x_k^{(u)}(1) \quad x_k^{(u)}(2) \quad \dots \quad x_k^{(u)}(N)]^T. \quad (8)$$

UE k transmits signal vector $\mathbf{x}_k^{(u)}$ with linear precoding matrix $\mathbf{V}_k^{(u)} \in \mathbb{C}^{N \times N}$ where

$$\mathbf{V}_k^{(u)} = [\mathbf{v}_k^{(u)}(1) \quad \mathbf{v}_k^{(u)}(2) \quad \dots \quad \mathbf{v}_k^{(u)}(N)]. \quad (9)$$

The i -th column vector of $\mathbf{V}_k^{(u)}$, $\mathbf{v}_k^{(u)}(i) \in \mathbb{C}^{N \times 1}$, is the precoding vector for signal $x_k^{(u)}(i)$ presented in (8).

With the N symbol extension of the channel, BS l observes received signal vector $\mathbf{y}_l^{(u)} \in \mathbb{C}^{N \times 1}$ where

$$\mathbf{y}_l^{(u)} = \sum_{k=1}^K \mathbf{H}_{l,k}^{(u)} \mathbf{V}_k^{(u)} \mathbf{x}_k^{(u)} + \mathbf{n}_l^{(u)}. \quad (10)$$

Diagonal channel matrix $\mathbf{H}_{l,k}^{(u)} \in \mathbb{C}^{N \times N}$ is an N symbol extension of channel coefficients where

$$\mathbf{H}_{l,k}^{(u)} = \text{diag} [h_{l,k}^{(u)}(1) \quad h_{l,k}^{(u)}(2) \quad \dots \quad h_{l,k}^{(u)}(N)] \quad (11)$$

and $h_{l,k}^{(u)}(i)$ is the CSI of the link from UE k to BS l in the i -th slot. Moreover, noise vector $\mathbf{n}_l^{(u)} \in \mathbb{C}^{N \times 1}$ is an N symbol extension of AWGN terms at BS l . The distribution of the noise vector is $\mathbf{n}_l^{(u)} \sim \mathcal{CN}(\mathbf{0}, (\sigma_l^{(u)})^2 \mathbf{I}_N)$, where $(\sigma_l^{(u)})^2 \mathbf{I}_N \in \mathbb{C}^{N \times N}$ is the noise covariance matrix.

BS l applies linear filtering matrix $\mathbf{U}_l^{(u)} \in \mathbb{C}^{N \times N}$ to received signal vector $\mathbf{y}_l^{(u)}$ where

$$\mathbf{U}_l^{(u)} = [\mathbf{u}_l^{(u)}(1) \quad \mathbf{u}_l^{(u)}(2) \quad \dots \quad \mathbf{u}_l^{(u)}(N)]. \quad (12)$$

The filtered signal vector at BS l is $\mathbf{y}_l'^{(u)} \in \mathbb{C}^{N \times 1}$ where

$$\begin{aligned} \mathbf{y}_l'^{(u)} &= (\mathbf{U}_l^{(u)})^H \mathbf{y}_l^{(u)} \\ &= \sum_{k=1}^K (\mathbf{U}_l^{(u)})^H \mathbf{H}_{l,k}^{(u)} \mathbf{V}_k^{(u)} \mathbf{x}_k^{(u)} + (\mathbf{U}_l^{(u)})^H \mathbf{n}_l^{(u)}. \end{aligned} \quad (13)$$

Then BS l demodulates filtered signal vector $\mathbf{y}_l'^{(u)}$ into demodulated message vector $\mathbf{b}_l'^{(u)} \in \mathbb{F}_q^{N \times 1}$.

Due to the page limit, here we describe the main idea for the downlink model, and the details can refer to the descriptions for the uplink model.

In the downlink, BS l receives the processed message vector $\tilde{\mathbf{b}}_l^{(d)} \in \mathbb{F}_q^{N \times 1}$ from the CP and modulates it to signal vector $\mathbf{x}_l^{(d)} \in \mathbb{C}^{N \times 1}$ over an N symbol extension where

$$\tilde{\mathbf{b}}_l^{(d)} = [\tilde{b}_l^{(d)}(1) \quad \tilde{b}_l^{(d)}(2) \quad \dots \quad \tilde{b}_l^{(d)}(N)]^T, \quad (14)$$

$$\mathbf{x}_l^{(d)} = [x_l^{(d)}(1) \quad x_l^{(d)}(2) \quad \dots \quad x_l^{(d)}(N)]^T. \quad (15)$$

BS l transmits signal vector $\mathbf{x}_l^{(d)}$ with linear precoding matrix $\mathbf{V}_l^{(d)} \in \mathbb{C}^{N \times N}$. Afterward, UE k decodes received signal vector $\mathbf{y}_k^{(d)} \in \mathbb{C}^{N \times 1}$ by linear filtering matrix $\mathbf{U}_k^{(d)} \in \mathbb{C}^{N \times N}$ to obtain filtered signal vector $\mathbf{y}_k'^{(d)} \in \mathbb{C}^{N \times 1}$ where

$$\mathbf{y}_k'^{(d)} = \sum_{l=1}^L (\mathbf{U}_k^{(d)})^H \mathbf{H}_{k,l}^{(d)} \mathbf{V}_l^{(d)} \mathbf{x}_l^{(d)} + (\mathbf{U}_k^{(d)})^H \mathbf{n}_k^{(d)}. \quad (16)$$

Finally, UE k demodulates filtered signal vector $\mathbf{y}_k'^{(d)}$ into demodulated message vector $\mathbf{b}_k^{(d)} \in \mathbb{F}_q^{N \times 1}$.

2) *BS-CP Links*: In the uplink, BS l forwards demodulated message vector $\mathbf{b}_l'^{(u)}$ to the CP through an independent noiseless digital link with a rate constraint $R_0 = \log_2(1 + \bar{\rho})$ where $\bar{\rho}$ denotes the average SNR of the UE-BS links. The CP collects all forwarded messages from the BSs and then recovers the original messages of the UEs. The recovered message vector of UE k is $\tilde{\mathbf{b}}_k^{(u)} \in \mathbb{F}_q^{N \times 1}$.

In the downlink, the CP wants to convey i.i.d. message vector $\mathbf{b}_k^{(d)} \in \mathbb{F}_q^{N \times 1}$ to UE k with the aid of the BSs where

$$\mathbf{b}_k^{(d)} = [b_k^{(d)}(1) \quad b_k^{(d)}(2) \quad \dots \quad b_k^{(d)}(N)]^T. \quad (17)$$

The CP passes the message vectors to a processing function $\omega(\cdot)$ where

$$(\tilde{\mathbf{b}}_1^{(d)}, \tilde{\mathbf{b}}_2^{(d)}, \dots, \tilde{\mathbf{b}}_L^{(d)}) = \omega(\mathbf{b}_1^{(d)}, \mathbf{b}_2^{(d)}, \dots, \mathbf{b}_K^{(d)}). \quad (18)$$

Then the CP assigns processed message vector $\tilde{\mathbf{b}}_l^{(d)}$ to BS l via an independent noiseless digital link with a restricted rate R_0 .

III. SIMPLE EXAMPLE

We present a simple example of the SNC scheme for the uplink and the downlink in this section. We consider there are two UEs and two BSs, i.e., $K = L = 2$. We also consider that each node has one antenna. We show that the users achieve total $d_{\text{sum}} = 5$ DoF over an $N = 3$ symbol extension in both the uplink and the downlink two-UE two-BS C-RANs by the

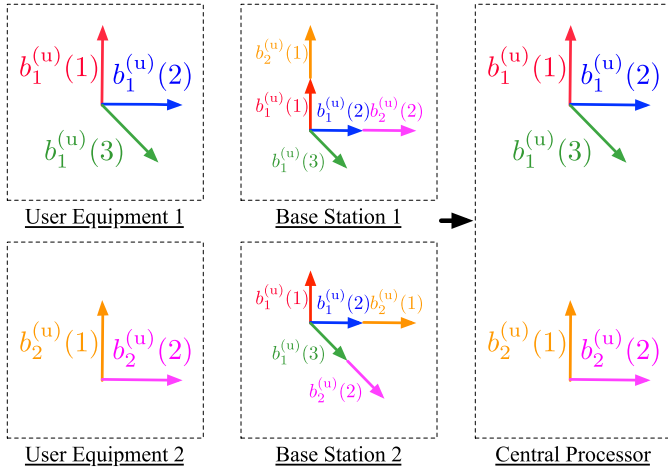


Fig. 2. A 3-dimensional vector diagram illustrating the SNC scheme in the two-UE two-BS uplink C-RAN.

SNC scheme. In this example, we describe the SNC scheme in terms of one supersymbol. We focus on the designs of the precoding matrices for signal alignment and the network coding operations for mitigating the interference. As the nodes are not sending only one supersymbol during the whole transmission, we can concatenate supersymbols to adopt error correction schemes.

A. Uplink

Fig. 2 shows the main idea of the SNC scheme in the two-UE two-BS uplink C-RAN, including the messages conveyed from the UEs, the network-coded messages decoded at the BSs, and the messages recovered at the CP. We assume that the CP can receive a network-coded symbol per slot from each BS concurrently. In Fig. 2, the arrows in the same direction mean that the signals conveying the corresponding messages are aligned. These aligned signals are then demodulated into network-coded messages. Now we describe the details of the example in this subsection.

UE 1 modulates message vector $\mathbf{b}_1^{(u)} = [b_1^{(u)}(1) \ b_1^{(u)}(2) \ b_1^{(u)}(3)]^T$ to signal vector $\mathbf{x}_1^{(u)} = [x_1^{(u)}(1) \ x_1^{(u)}(2) \ x_1^{(u)}(3)]^T$ while UE 2 modulates message vector $\mathbf{b}_2^{(u)} = [b_2^{(u)}(1) \ b_2^{(u)}(2)]^T$ to signal vector $\mathbf{x}_2^{(u)} = [x_2^{(u)}(1) \ x_2^{(u)}(2)]^T$. Afterward, UE $k \in \{1, 2\}$ transmits signal vector $\mathbf{x}_k^{(u)}$ with linear precoding matrix $\mathbf{V}_k^{(u)}$. The received signal vector at BS $l \in \{1, 2\}$ is

$$\mathbf{y}_l^{(u)} = \mathbf{H}_{l,1}^{(u)} \mathbf{V}_1^{(u)} \mathbf{x}_1^{(u)} + \mathbf{H}_{l,2}^{(u)} \mathbf{V}_2^{(u)} \mathbf{x}_2^{(u)} + \mathbf{n}_l^{(u)}. \quad (19)$$

In order to achieve the ideas of the SNC scheme, we can set the linear precoding matrices of the UEs as

$$\mathbf{V}_1^{(u)} = \begin{bmatrix} (\mathbf{G}_{1,2}^{(u)})^2 \mathbf{w} & (\mathbf{G}_{1,2}^{(u)}) (\mathbf{G}_{2,2}^{(u)}) \mathbf{w} & (\mathbf{G}_{2,2}^{(u)})^2 \mathbf{w} \end{bmatrix}, \quad (20)$$

$$\mathbf{V}_2^{(u)} = \begin{bmatrix} (\mathbf{G}_{1,2}^{(u)}) \mathbf{w} & (\mathbf{G}_{2,2}^{(u)}) \mathbf{w} \end{bmatrix} \quad (21)$$

where $\mathbf{G}_{1,2}^{(u)} = (\mathbf{H}_{1,1}^{(u)})^{-1} (\mathbf{H}_{1,2}^{(u)})$, $\mathbf{G}_{2,2}^{(u)} = (\mathbf{H}_{2,1}^{(u)})^{-1} (\mathbf{H}_{2,2}^{(u)})$, and $\mathbf{w} = [1 \ 1 \ 1]^T$. $\mathbf{V}_1^{(u)}$ consists of 3 column vectors, namely $(\mathbf{G}_{1,2}^{(u)})^2 \mathbf{w}$, $(\mathbf{G}_{1,2}^{(u)}) (\mathbf{G}_{2,2}^{(u)}) \mathbf{w}$, and $(\mathbf{G}_{2,2}^{(u)})^2 \mathbf{w}$. The composition of $\mathbf{V}_2^{(u)}$ can be understood likewise.

Now we describe how the linear precoding matrices of the UEs affect the messages decoded at the BSs specifically. As the multiplications of diagonal matrices are commutative, the multiplications of the channel matrices and the linear precoding matrices at BS 1 are

$$\begin{aligned} & \mathbf{H}_{1,1}^{(u)} \mathbf{V}_1^{(u)} \\ &= \begin{bmatrix} (\mathbf{H}_{1,2}^{(u)}) (\mathbf{G}_{1,2}^{(u)}) \mathbf{w} & (\mathbf{H}_{1,2}^{(u)}) (\mathbf{G}_{2,2}^{(u)}) \mathbf{w} & (\mathbf{H}_{1,1}^{(u)}) (\mathbf{G}_{2,2}^{(u)})^2 \mathbf{w} \end{bmatrix} \text{ and} \end{aligned} \quad (22)$$

$$\begin{aligned} & \mathbf{H}_{1,2}^{(u)} \mathbf{V}_2^{(u)} \\ &= \begin{bmatrix} (\mathbf{H}_{1,2}^{(u)}) (\mathbf{G}_{1,2}^{(u)}) \mathbf{w} & (\mathbf{H}_{1,2}^{(u)}) (\mathbf{G}_{2,2}^{(u)}) \mathbf{w} \end{bmatrix}. \end{aligned} \quad (23)$$

The first column vector of $\mathbf{H}_{1,1}^{(u)} \mathbf{V}_1^{(u)}$, which is $(\mathbf{H}_{1,2}^{(u)}) (\mathbf{G}_{1,2}^{(u)}) \mathbf{w}$, for signal $x_1^{(u)}(1)$ is the same as the first column vector of $\mathbf{H}_{1,2}^{(u)} \mathbf{V}_2^{(u)}$ for signal $x_2^{(u)}(1)$. A similar relationship holds between signals $x_1^{(u)}(2)$ and $x_2^{(u)}(2)$ at BS 1. BS 1 decodes received signal vector $\mathbf{y}_1^{(u)}$ by linear filtering matrix $(\mathbf{U}_1^{(u)})^H = (\mathbf{H}_{1,1}^{(u)} \mathbf{V}_1^{(u)})^{-1}$. The filtered signal vector $\mathbf{y}'_1^{(u)}$ would be

$$\begin{aligned} \mathbf{y}'_1^{(u)} &= (\mathbf{U}_1^{(u)})^H \mathbf{y}_1^{(u)} \\ &= (\mathbf{U}_1^{(u)})^H \mathbf{H}_{1,1}^{(u)} \mathbf{V}_1^{(u)} \mathbf{x}_1^{(u)} + (\mathbf{U}_1^{(u)})^H \mathbf{H}_{1,2}^{(u)} \mathbf{V}_2^{(u)} \mathbf{x}_2^{(u)} \\ &\quad + (\mathbf{U}_1^{(u)})^H \mathbf{n}_1^{(u)}. \end{aligned} \quad (24)$$

As the first two column vectors of $\mathbf{H}_{1,1}^{(u)} \mathbf{V}_1^{(u)}$ are the same as the column vectors of $\mathbf{H}_{1,2}^{(u)} \mathbf{V}_2^{(u)}$, we can express filtered signal vector $\mathbf{y}'_1^{(u)}$ as

$$\mathbf{y}'_1^{(u)} = \begin{bmatrix} x_1^{(u)}(1) + x_2^{(u)}(1) & x_1^{(u)}(2) + x_2^{(u)}(2) & x_1^{(u)}(3) \end{bmatrix}^T + (\mathbf{U}_1^{(u)})^H \mathbf{n}_1^{(u)}. \quad (25)$$

We treat the aligned signal (e.g. $x_1^{(u)}(1) + x_2^{(u)}(1)$) as an unknown for demodulation rather than demodulate the original signals (e.g. $x_1^{(u)}(1)$ and $x_2^{(u)}(1)$) individually by PNC demodulation. We demodulate the aligned signal (e.g. $x_1^{(u)}(1) + x_2^{(u)}(1)$) into an linear combination of the transmitted messages (e.g. $b_1^{(u)}(1) \oplus b_2^{(u)}(1)$) over the same finite field as the conveyed messages, without distinguishing each individual message (e.g. $b_1^{(u)}(1)$ and $b_2^{(u)}(1)$). The idea of PNC demodulation [6] also applies in the rest of this paper. This idea can be achieved explicitly by compute-and-forward or other PNC strategies. From an information-theoretic aspect, the framework of compute-and-forward [19] generalize the concept of PNC with multiple nodes. Nested lattice codes are used to prove the information-theoretic results. In this paper, we adopt the fundamental framework of compute and forward described in [19] in which superimposed signals are decoded into an integer combination of the codewords utilizing the nested lattice code. We refer the details of the compute-and-forward coding scheme to [19]. As a result, BS 1 demodulates filtered signal vectors $\mathbf{y}'_1^{(u)}$ into network-coded message

vector

$$\begin{aligned} \mathbf{b}'_1^{(u)} &= \left[b_1^{(u)}(1) \oplus b_2^{(u)}(1) \quad b_1^{(u)}(2) \oplus b_2^{(u)}(2) \quad b_1^{(u)}(3) \right]^T \\ &= \begin{bmatrix} 1 & 0 & 0 & 1 & 0 \\ 0 & 1 & 0 & 0 & 1 \\ 0 & 0 & 1 & 0 & 0 \end{bmatrix} \otimes \left[b_1^{(u)}(1), b_1^{(u)}(2), b_1^{(u)}(3), b_2^{(u)}(1), b_2^{(u)}(2) \right]^T \\ &= \mathbf{F}_1^{(u)} \otimes \left[b_1^{(u)}(1) \quad b_1^{(u)}(2) \quad b_1^{(u)}(3) \quad b_2^{(u)}(1) \quad b_2^{(u)}(2) \right]^T \quad (26) \end{aligned}$$

where $\mathbf{F}_1^{(u)} \in \mathbb{F}_q^{3 \times 5}$ is the alignment matrix of BS 1.

Afterward, we look at the signals filtered and demodulated at BS 2. BS 2 decodes received signal vector $\mathbf{y}_2^{(u)}$ through linear filtering matrix $(\mathbf{U}_2^{(u)})^H = (\mathbf{H}_{2,1}^{(u)} \mathbf{V}_1^{(u)})^{-1}$. The filtered signal vector $\mathbf{y}'_2^{(u)}$ is

$$\begin{aligned} \mathbf{y}'_2^{(u)} &= (\mathbf{U}_2^{(u)})^H \mathbf{y}_2^{(u)} \\ &= (\mathbf{U}_2^{(u)})^H \mathbf{H}_{2,1}^{(u)} \mathbf{V}_1^{(u)} \mathbf{x}_1^{(u)} + (\mathbf{U}_2^{(u)})^H \mathbf{H}_{2,2}^{(u)} \mathbf{V}_2^{(u)} \mathbf{x}_2^{(u)} \\ &\quad + (\mathbf{U}_2^{(u)})^H \mathbf{n}_2^{(u)}. \quad (27) \end{aligned}$$

As the multiplications of diagonal matrices are commutative, the multiplications of the channel matrices and the linear precoding matrices at BS 2 are

$$\begin{aligned} \mathbf{H}_{2,1}^{(u)} \mathbf{V}_1^{(u)} &= \left[(\mathbf{H}_{2,1}^{(u)}) (\mathbf{G}_{1,2}^{(u)})^2 \mathbf{w} \quad (\mathbf{H}_{2,2}^{(u)}) (\mathbf{G}_{1,2}^{(u)}) \mathbf{w} \quad (\mathbf{H}_{2,2}^{(u)}) (\mathbf{G}_{2,2}^{(u)}) \mathbf{w} \right] \text{ and} \\ &\quad (28) \end{aligned}$$

$$\begin{aligned} \mathbf{H}_{2,2}^{(u)} \mathbf{V}_2^{(u)} &= \left[(\mathbf{H}_{2,2}^{(u)}) (\mathbf{G}_{1,2}^{(u)}) \mathbf{w} \quad (\mathbf{H}_{2,2}^{(u)}) (\mathbf{G}_{2,2}^{(u)}) \mathbf{w} \right]. \quad (29) \end{aligned}$$

BS 2 then demodulates filtered signal vector $\mathbf{y}'_2^{(u)}$ into network-coded message vector

$$\begin{aligned} \mathbf{b}'_2^{(u)} &= \left[b_1^{(u)}(1) \quad b_1^{(u)}(2) \oplus b_2^{(u)}(1) \quad b_1^{(u)}(3) \oplus b_2^{(u)}(2) \right] \\ &= \begin{bmatrix} 1 & 0 & 0 & 0 & 0 \\ 0 & 1 & 0 & 1 & 0 \\ 0 & 0 & 1 & 0 & 1 \end{bmatrix} \otimes \left[b_1^{(u)}(1), b_1^{(u)}(2), b_1^{(u)}(3), b_2^{(u)}(1), b_2^{(u)}(2) \right]^T \\ &= \mathbf{F}_2^{(u)} \otimes \left[b_1^{(u)}(1) \quad b_1^{(u)}(2) \quad b_1^{(u)}(3) \quad b_2^{(u)}(1) \quad b_2^{(u)}(2) \right]^T \quad (30) \end{aligned}$$

where $\mathbf{F}_2^{(u)} \in \mathbb{F}_q^{3 \times 5}$ is the alignment matrix of BS 2.

The CP collects network-coded message vectors $\mathbf{b}'_1^{(u)}$ and $\mathbf{b}'_2^{(u)}$ forwarded from BS 1 and 2, respectively, via the independent noiseless digital links. Note that the BSs obtain messages from the UEs and forward the network-coded messages received at the previous slot to the CP concurrently. The CP can recover all original messages of the UEs by solving any 5 independent equations with 5 unknowns. As a result, the users achieve a total of $\frac{5}{3}$ DoF per slot in two-UE two-BS uplink C-RAN by the SNC scheme.

In this example, UE 2 cannot convey $b_2^{(u)}(3)$ while the alignment matrix of the system $\mathbf{F}^{(u)}$ keeps always having full rank over $\text{GF}(q)$. Without signal alignment, there exists the rank deficiency problem described in [19], [22]. Performing signal alignment, the only solution for the precoding vectors

to align at least 6 pairs of signals is being zero vectors. Hence, we cannot align the signals in this way. However, we can simply extend our SNC scheme with a sufficiently large number of symbol extension N so that the users achieve a total of $\frac{N+(N-1)}{N} \rightarrow 2$ DoF per slot asymptotically. The details can be found in Section IV.

B. Downlink

In the downlink, we exchange the roles of the UEs and the BSs, i.e., the BSs are the transmitters while the UEs are the receivers. We assume that the CP can transmit a network-coded symbol per slot to each BS concurrently. The signals in the wireless links are aligned as in the uplink case, which means alignment matrices $\mathbf{F}_1^{(d)} = \mathbf{F}_1^{(u)}$ and $\mathbf{F}_2^{(d)} = \mathbf{F}_2^{(u)}$. The setup of the precoding matrices of BSs is omitted to avoid repetition. The demodulated network-coded message vectors at UEs 1 and 2 in the second transmission phase (BS-UE communications) are

$$\begin{aligned} \mathbf{b}'_k^{(d)} &= \mathbf{F}_k^{(d)} \otimes \left[\tilde{b}_1^{(d)}(1) \quad \tilde{b}_1^{(d)}(2) \quad \tilde{b}_1^{(d)}(3) \quad \tilde{b}_2^{(d)}(1) \quad \tilde{b}_2^{(d)}(2) \right]^T \\ &\quad \forall k \in \{1, 2\}. \quad (31) \end{aligned}$$

Recall that the CP wants to convey message vectors $\left[b_1^{(d)}(1) \quad b_1^{(d)}(2) \quad b_1^{(d)}(3) \right]^T$ and $\left[b_2^{(d)}(1) \quad b_2^{(d)}(2) \right]^T$ to UEs 1 and 2, respectively, with the aid of the BSs. We now consider the messages processed at the CP in the first transmission phase (CP-BS communications). We combine the alignment matrices of UEs 1 and 2 and form an alignment matrix of the system where

$$\begin{aligned} \mathbf{F}^{(d)} &= \begin{bmatrix} \mathbf{F}_1^{(d)} & \mathbf{F}_2^{(d)} \end{bmatrix}^T \\ &= \begin{bmatrix} 1 & 0 & 0 & 1 & 0 \\ 0 & 1 & 0 & 0 & 1 \\ 0 & 0 & 1 & 0 & 0 \\ 1 & 0 & 0 & 0 & 0 \\ 0 & 1 & 0 & 1 & 0 \\ 0 & 0 & 1 & 0 & 1 \end{bmatrix}. \quad (32) \end{aligned}$$

Afterward, we select the first five rows of $\mathbf{F}^{(d)}$ to form an invertible matrix $\mathbf{F}'^{(d)}$.

The CP left-multiplies the message vectors for the UEs by the inverse of $\mathbf{F}'^{(d)}$ to generate the processed message vectors, i.e.,

$$\begin{aligned} &\left[\tilde{b}_1^{(d)}(1) \quad \tilde{b}_1^{(d)}(2) \quad \tilde{b}_1^{(d)}(3) \quad \tilde{b}_2^{(d)}(1) \quad \tilde{b}_2^{(d)}(2) \right]^T \\ &= (\mathbf{F}'^{(d)})^{-1} \otimes \left[b_1^{(d)}(1) \quad b_1^{(d)}(2) \quad b_1^{(d)}(3) \quad b_2^{(d)}(1) \quad b_2^{(d)}(2) \right]^T \\ &= \begin{bmatrix} 0 & 0 & 0 & 1 & 0 \\ 1 & 0 & 0 & 1 & 1 \\ 0 & 0 & 1 & 0 & 0 \\ 1 & 0 & 0 & 1 & 0 \\ 1 & 1 & 0 & 1 & 1 \end{bmatrix} \otimes \begin{bmatrix} b_1^{(d)}(1) \\ b_1^{(d)}(2) \\ b_1^{(d)}(3) \\ b_2^{(d)}(1) \\ b_2^{(d)}(2) \end{bmatrix} \quad (33) \end{aligned}$$

Then the CP assigns processed message vectors $\left[\tilde{b}_1^{(d)}(1) \quad \tilde{b}_1^{(d)}(2) \quad \tilde{b}_1^{(d)}(3) \right]^T$ and $\left[\tilde{b}_2^{(d)}(1) \quad \tilde{b}_2^{(d)}(2) \right]^T$ to BS 1 and BS 2, respectively, via the digital links.

Finally, we show how the interfering messages are canceled with each other at each UE by the proper messages processing at the CP. According to (31) and (33), UE 1 obtains demodulated messages

$$\begin{aligned}
& \mathbf{b}_1^{(d)} \\
&= \mathbf{F}_1^{(d)} \otimes (\mathbf{F}'^{(d)})^{-1} \otimes [b_1^{(d)}(1), b_1^{(d)}(2), b_1^{(d)}(3), b_2^{(d)}(1), b_2^{(d)}(2)]^T \\
&= \begin{bmatrix} 1 & 0 & 0 & 1 & 0 \\ 0 & 1 & 0 & 0 & 1 \\ 0 & 0 & 1 & 0 & 0 \end{bmatrix} \otimes \begin{bmatrix} 0 & 0 & 0 & 1 & 0 \\ 1 & 0 & 0 & 1 & 1 \\ 0 & 0 & 1 & 0 & 0 \\ 1 & 0 & 0 & 1 & 0 \\ 1 & 1 & 0 & 1 & 1 \end{bmatrix} \otimes \begin{bmatrix} b_1^{(d)}(1) \\ b_1^{(d)}(2) \\ b_1^{(d)}(3) \\ b_2^{(d)}(1) \\ b_2^{(d)}(2) \end{bmatrix} \\
&= \begin{bmatrix} 1 & 0 & 0 & 0 & 0 \\ 0 & 1 & 0 & 0 & 0 \\ 0 & 0 & 1 & 0 & 0 \end{bmatrix} \otimes [b_1^{(d)}(1), b_1^{(d)}(2), b_1^{(d)}(3), b_2^{(d)}(1), b_2^{(d)}(2)]^T \\
&= [b_1^{(d)}(1) \quad b_1^{(d)}(2) \quad b_1^{(d)}(3)]^T. \tag{34}
\end{aligned}$$

According to (31) and (33), UE 2 can obtain the desired messages without interference likewise.

As a result, the users achieve total $\frac{5}{3}$ DoF per slot in two-UE two-BS downlink C-RAN by the SNC scheme. As in the uplink case, we can simply extend this example with a sufficiently large number of symbol extension, and the users can achieve a total of 2 DoF per slot asymptotically. The details can be found in the next section.

IV. SIGNAL-ALIGNED NETWORK CODING

We describe the details of the SNC scheme in this section. Here we consider that the numbers of the UEs and the BSs are equal, i.e., $K = L$. We also consider that each node is equipped with one antenna. Appendix A presents the general SNC scheme for MIMO cases with arbitrary numbers of UEs, BSs, and antennas of each node. We denote $N = \binom{n+K(K-1)-1}{n}$ and $N' = \binom{n+K(K-1)-2}{n-1}$ where symbol extension parameter $n \in \mathbb{Z}^+$ and $K \geq 2$. We use UE $k' \in \{2, 3, \dots, K\}$ to indicate each UE except UE 1. We also use BS $l' \in \{2, 3, \dots, L\}$ to indicate each BS except BS 1.

The system adopts an N symbol extension. In this section, we show that DoF tuple (d_1, d_2, \dots, d_K) per slot is achievable where

$$d_1 = \frac{N}{N} = 1 \quad \text{and} \tag{35}$$

$$d_{k'} = \frac{N'}{N} = \frac{n}{n + K(K-1) - 1} \quad \forall k' \in \{2, 3, \dots, K\}. \tag{36}$$

Moreover,

$$\sup_n \left(\frac{N}{N} + (K-1) \frac{N'}{N} \right) = \sup_n \frac{Kn + K(K-1) - 1}{n + K(K-1) - 1} = K. \tag{37}$$

A. Uplink

The SNC scheme for the uplink aligns the signals of the UEs at each BS so that the BSs obtain independent linear combinations of messages over $\text{GF}(q)$, also known as network-coded messages. The CP then recovers all original messages of the UEs by solving the linearly independent equations. Now we describe the SNC scheme for the uplink in detail.

UE 1 modulates $N \times 1$ message vector $\mathbf{b}_1^{(u)}$ to $N \times 1$ signal vector $\mathbf{x}_1^{(u)}$ while UE k' modulates $N' \times 1$ message vector $\mathbf{b}_{k'}^{(u)}$ to $N' \times 1$ signal vector $\mathbf{x}_{k'}^{(u)}$. Then UE 1 transmits signal vector $\mathbf{x}_1^{(u)}$ with $N \times N$ linear precoding matrix $\mathbf{V}_1^{(u)}$ while UE k' transmits signal vector $\mathbf{x}_{k'}^{(u)}$ with $N \times N'$ linear precoding matrix $\mathbf{V}_{k'}^{(u)}$. The $N \times 1$ received signal vector at BS $l \in \{1, 2, \dots, K\}$ is

$$\mathbf{y}_l^{(u)} = \sum_{k=1}^K \mathbf{H}_{l,k}^{(u)} \mathbf{V}_k^{(u)} \mathbf{x}_k^{(u)} + \mathbf{n}_l^{(u)}. \tag{38}$$

We set up the following signal alignment constraints for the UEs:

$$\mathbf{H}_{l,k'}^{(u)} \mathbf{V}_{k'}^{(u)} \prec \mathbf{H}_{l,1}^{(u)} \mathbf{V}_1^{(u)} \quad \forall l \in \{1, 2, \dots, L\} \quad \forall k' \in \{2, 3, \dots, K\} \tag{39}$$

where $\mathbf{Q} \prec \mathbf{P}$ denotes the column vectors of matrix \mathbf{Q} is a subset of those of matrix \mathbf{P} . In order to fulfill alignment constraints (39) and the ideas of the SNC scheme, we set up the linear precoding matrices of the UEs according to the following way. The sets of the column vectors of $\mathbf{V}_1^{(u)}$ and $\mathbf{V}_{k'}^{(u)}$ are equal to the set $V_1^{(u)}$ and $V_{k'}^{(u)}$ respectively. Here

$$V_1^{(u)} = \left\{ \left(\prod_{\substack{i \in \{1, 2, \dots, L\}, \\ j \in \{2, 3, \dots, K\}}} (\mathbf{G}_{i,j}^{(u)})^{n_{i,j}} \right) \mathbf{w} : \sum_{i,j} n_{i,j} = n, n_{i,j} \in \mathbb{Z} \right\} \tag{40}$$

and

$$V_{k'}^{(u)} = \left\{ \left(\prod_{\substack{i \in \{1, 2, \dots, L\}, \\ j \in \{2, 3, \dots, K\}}} (\mathbf{G}_{i,j}^{(u)})^{n_{i,j}} \right) \mathbf{w} : \sum_{i,j} n_{i,j} = n - 1, n_{i,j} \in \mathbb{Z} \right\} \quad \forall k' \in \{2, 3, \dots, K\} \tag{41}$$

where $\mathbf{G}_{i,j}^{(u)} = (\mathbf{H}_{i,1}^{(u)})^{-1} (\mathbf{H}_{i,j}^{(u)})$ and \mathbf{w} is an arbitrary $N \times 1$ column vector. Without loss of generality, we assume $\mathbf{w} = [1 \quad 1 \quad \dots \quad 1]^T$ in this section. As a result, the signals from the UEs are aligned at each BS. We take BS 1 as an example. The column vectors of matrix $\mathbf{H}_{1,k'}^{(u)} \mathbf{V}_{k'}^{(u)}$ is a subset of those of matrix $\mathbf{H}_{1,1}^{(u)} \mathbf{V}_1^{(u)}$. Hence, the signals from all UEs are aligned at BS 1. Likewise, any column vector in $\mathbf{H}_{l,k'}^{(u)} \mathbf{V}_{k'}^{(u)}$ can be found in $\mathbf{H}_{l,1}^{(u)} \mathbf{V}_1^{(u)}$.

Lemma 1: Linear precoding matrix $\mathbf{V}_1^{(u)}$ and $\mathbf{V}_{k'}^{(u)}$ has rank N and N' respectively.

The proof of Lemma 1 is presented in Appendix B.

BS l applies $N \times N$ linear filtering matrix $(\mathbf{U}_l^{(u)})^H$ to $N \times 1$ received signal vector $\mathbf{y}_l^{(u)}$. As the elements of channel matrix $\mathbf{H}_{l,1}^{(u)}$ are drawn independently from a continuous distribution and linear precoding matrix $\mathbf{V}_1^{(u)}$ is invertible, matrix $\mathbf{H}_{l,1}^{(u)}\mathbf{V}_1^{(u)}$ is invertible almost certainly. For the sake of simplicity, we assume BS l applies zero-forcing such that $(\mathbf{U}_l^{(u)})^H = (\mathbf{H}_{l,1}^{(u)}\mathbf{V}_1^{(u)})^{-1}$ in this section. The $N \times 1$ filtered signal vector at BS l is

$$\begin{aligned} \mathbf{y}_l^{\prime(u)} &= (\mathbf{U}_l^{(u)})^H \mathbf{y}_l^{(u)} \\ &= \sum_{k=1}^K (\mathbf{U}_l^{(u)})^H \mathbf{H}_{l,k}^{(u)} \mathbf{V}_k^{(u)} \mathbf{x}_k^{(u)} + (\mathbf{U}_l^{(u)})^H \mathbf{n}_l^{(u)}. \end{aligned} \quad (42)$$

Therefore, the effective channel matrix of the system is (43), as shown at the bottom of this page. The effective channel for transmitting signal $x_k^{(u)}(i)$ from UE k to BS l is the entry $\mathbf{u}_l^{(u)}(j)\mathbf{H}_{l,k}^{(u)}\mathbf{v}_k^{(u)}(i)$ in $\tilde{\mathbf{F}}^{(u)}$.

Filtered signal vector $\mathbf{y}_l^{\prime(u)}$ is then demodulated into network-coded message $\mathbf{b}_l^{\prime(u)}$. This idea of PNC demodulation [6] can be achieved explicitly by compute-and-forward or other PNC strategies. As we focus on the information-theoretic rates of the SNC scheme in this paper, we adopt the fundamental framework of compute-and-forward described in [19] in which superimposed signals are decoded into an integer combination of the codewords utilizing the nested lattice code.

The CP pools $N \times 1$ network-coded message vectors $\mathbf{b}_l^{\prime(u)}$ forwarded from BS l via the independent noiseless digital links and forms $KN \times 1$ network-coded message vector $\mathbf{b}_c^{\prime(u)}$ where

$$\begin{aligned} \mathbf{b}_c^{\prime(u)} &= [\mathbf{b}_1^{\prime(u)} \quad \mathbf{b}_2^{\prime(u)} \quad \dots \quad \mathbf{b}_L^{\prime(u)}]^T \\ &= \mathbf{F}^{(u)} \otimes [\mathbf{b}_1^{(u)} \quad \mathbf{b}_2^{(u)} \quad \dots \quad \mathbf{b}_K^{(u)}]^T, \end{aligned} \quad (44)$$

where $\mathbf{F}^{(u)}$ denotes the $KN \times [N + (K-1)N']$ alignment matrix of the uplink system over $\text{GF}(q)$. Intuitively, the alignment matrix $\mathbf{F}^{(u)}$ can also be treated as the binary matrix $\tilde{\mathbf{F}}^{(u)}$ stated in (43) over $\text{GF}(q)$. Section III provided concrete examples to show the relationship between the alignment matrix for the conveyed messages $\mathbf{F}^{(u)}$ and the effective channel matrix for the transmitted signals $\tilde{\mathbf{F}}^{(u)}$.

Lemma 2: Alignment matrix of the system $\mathbf{F}^{(u)}$ has rank $N + (K-1)N'$ for some finite field sizes q .

The proof of Lemma 2 is presented in Appendix C. As a result, there exists $N + (K-1)N'$ independent linear combinations of messages over $\text{GF}(q)$ with $N + (K-1)N'$ unknown messages collected by the CP. The CP can recover all original messages of the UEs by solving the independent equations

without the rank deficiency problem. Therefore, the users achieve total $N + (K-1)N'$ DoF over an N symbol extension in the uplink by the SNC scheme. As stated in (37), K DoF per slot can be achieved asymptotically by the SNC scheme, equivalent to unlimited cooperation at the BS side to form K parallel interference-free channels. This asymptotic full DoF achievement is not limited by the number of antennas of each node.

B. Downlink

The SNC scheme for the downlink appropriately designs the network-coded messages conveyed from the CP to the BSs and aligns the signals from the BSs at each UE so that the interfering signals are canceled with each other during PNC demodulation.

In the downlink, the BSs are the transmitters while the UEs are the receivers. The signals in the wireless links are aligned as in the uplink case. In other words, we can form the alignment matrix of the system in the downlink $\mathbf{F}^{(d)} = \mathbf{F}^{(u)}$. The descriptions of the precoding matrices of BSs are omitted to avoid repetition.

Recall that the $KN \times [N + (K-1)N']$ alignment matrix of the system $\mathbf{F}^{(d)}$ has rank $N + (K-1)N'$, and

$$\mathbf{F}^{(d)} = [\mathbf{F}_1^{(d)} \quad \mathbf{F}_2^{(d)} \quad \dots \quad \mathbf{F}_K^{(d)}]^T. \quad (45)$$

We can pick N independent rows from $\mathbf{F}_1^{(d)}$ and N' independent rows from $\mathbf{F}_{k'}^{(d)}$, where $k' \in \{2, 3, \dots, K\}$, to form an $(N + (K-1)N') \times (N + (K-1)N')$ invertible matrix $\mathbf{F}'^{(d)}$. As $\mathbf{F}'^{(d)}$ has a similar structure to $\mathbf{F}^{(d)}$, $\mathbf{F}'^{(d)}$ can be proved to have rank $N + (K-1)N'$ likewise. The proof is omitted to avoid repetition.

In order to let the UEs obtain their intended message vector without interference, the CP processes the messages of the UEs by left-multiplying them by the inverse of $\mathbf{F}'^{(d)}$. The processed message vectors at the CP are

$$\begin{aligned} &[\tilde{\mathbf{b}}_1^{(d)} \quad \tilde{\mathbf{b}}_2^{(d)} \quad \dots \quad \tilde{\mathbf{b}}_L^{(d)}]^T \\ &= (\mathbf{F}'^{(d)})^{-1} \otimes [\mathbf{b}_1^{(d)} \quad \mathbf{b}_2^{(d)} \quad \dots \quad \mathbf{b}_K^{(d)}]^T. \end{aligned} \quad (46)$$

Afterward, the CP assigns processed message vectors $\tilde{\mathbf{b}}_l^{(d)}$ to BS l through an independent noiseless digital link. The received message vector at UE $k \in \{1, 2, \dots, K\}$ is

$$\begin{aligned} \mathbf{b}_k^{\prime(d)} &= \mathbf{F}_k^{(d)} \otimes [\tilde{\mathbf{b}}_1^{(d)} \quad \tilde{\mathbf{b}}_2^{(d)} \quad \dots \quad \tilde{\mathbf{b}}_L^{(d)}]^T \\ &= \mathbf{F}_k^{(d)} \otimes (\mathbf{F}'^{(d)})^{-1} \otimes [\mathbf{b}_1^{(d)} \quad \mathbf{b}_2^{(d)} \quad \dots \quad \mathbf{b}_K^{(d)}]^T \\ &= \mathbf{b}_k^{(d)}. \end{aligned} \quad (47)$$

$$\tilde{\mathbf{F}}^{(u)} = \begin{bmatrix} (\mathbf{U}_1^{(u)})^H \mathbf{H}_{1,1}^{(u)} \mathbf{V}_1^{(u)} & (\mathbf{U}_1^{(u)})^H \mathbf{H}_{1,2}^{(u)} \mathbf{V}_2^{(u)} & \dots & (\mathbf{U}_1^{(u)})^H \mathbf{H}_{1,K}^{(u)} \mathbf{V}_K^{(u)} \\ (\mathbf{U}_2^{(u)})^H \mathbf{H}_{2,1}^{(u)} \mathbf{V}_1^{(u)} & (\mathbf{U}_2^{(u)})^H \mathbf{H}_{2,2}^{(u)} \mathbf{V}_2^{(u)} & \dots & (\mathbf{U}_2^{(u)})^H \mathbf{H}_{2,K}^{(u)} \mathbf{V}_K^{(u)} \\ \vdots & \vdots & \ddots & \vdots \\ (\mathbf{U}_L^{(u)})^H \mathbf{H}_{L,1}^{(u)} \mathbf{V}_1^{(u)} & (\mathbf{U}_L^{(u)})^H \mathbf{H}_{L,2}^{(u)} \mathbf{V}_2^{(u)} & \dots & (\mathbf{U}_L^{(u)})^H \mathbf{H}_{L,K}^{(u)} \mathbf{V}_K^{(u)} \end{bmatrix}. \quad (43)$$

All UEs can obtain their intended messages without interference because of the relationships between $\mathbf{F}_k^{(d)}$ and $(\mathbf{F}'^{(d)})^{-1}$. For ease of explanation, Section III presents a concrete two-user example with a 3 symbol extension.

As a result, the users achieve total $N + (K - 1)N'$ DoF over an N symbol extension in the downlink by the SNC scheme. The sum DoF achieved per slot tends to K with a large value of symbol extension parameter n , equivalent to unlimited cooperation at the BS side to form K parallel interference-free channels. This asymptotic full DoF achievement is not limited by the number of antennas of each node.

C. End-to-End Sum-Rate

We present the end-to-end sum-rate of the SNC scheme in this subsection. First, we consider the achievable rate of the UE-BS link.

Proposition 1: According to [19, Example 1], the achievable rate of transmitting signal $x_k^{(u)}(i)$ from UE k to BSs in the uplink by the SNC scheme is (48), as shown at the bottom of this page, bits per channel use. The achievable rate of transmitting signal $x_l^{(d)}(i)$ from BS l to UEs in the downlink, $R_l^{(d)}(i)$, can be found likewise.

Proof: We first describe the notations used in (48). Here we focus on the uplink case. Recall that the entries in the effective channel matrix $\tilde{\mathbf{F}}^{(u)}$ can be expressed as $\mathbf{u}_l^{(u)}(j)\mathbf{H}_{l,k}^{(u)}\mathbf{v}_k^{(u)}(i)$, which is the effective channel for transmitting signal $x_k^{(u)}(i)$ from UE k to BS l . We define $\tilde{f}^{(u)}(a, b)$ be the (a, b) -th entry of the effective channel matrix $\tilde{\mathbf{F}}^{(u)}$. The vector $\tilde{\mathbf{f}}^{(u)}(a, :)$ denotes the a -th row of the effective channel matrix $\tilde{\mathbf{F}}^{(u)}$. Moreover, the vector $\tilde{\mathbf{f}}^{(u)}(:, b)$ denotes the b -th column of the effective channel matrix $\tilde{\mathbf{F}}^{(u)}$.

We define the following notations for the filtering vector $\mathbf{u}_l^{(u)}(i)$, channel matrix $\mathbf{H}_{l,k}^{(u)}$, and precoding vector $\mathbf{v}_k^{(u)}(j)$ in the entry $\tilde{f}^{(u)}(a, b)$. The filtering vector in the entry $\tilde{f}^{(u)}(a, b)$ is

$$\mathbf{u}_{\tilde{f}^{(u)}(a,b)}^{(u)} = \mathbf{u}_{\lceil \frac{a}{N} \rceil}^{(u)}(a - (\lceil \frac{a}{N} \rceil - 1)N). \quad (49)$$

The channel matrix in the entry $\tilde{f}^{(u)}(a, b)$ is

$$\mathbf{H}_{\tilde{f}^{(u)}(a,b)}^{(u)} = \begin{cases} \mathbf{H}_{\lceil \frac{a}{N} \rceil, 1}^{(u)} & \text{if } b \leq N, \\ \mathbf{H}_{\lceil \frac{a}{N} \rceil, \lceil \frac{b-N}{N'} \rceil + 1}^{(u)} & \text{otherwise.} \end{cases} \quad (50)$$

The precoding vector in the entry $\tilde{f}^{(u)}(a, b)$ is

$$\mathbf{v}_{\tilde{f}^{(u)}(a,b)}^{(u)} = \begin{cases} \mathbf{v}_1^{(u)}(b) & \text{if } b \leq N, \\ \mathbf{v}_{\lceil \frac{b-N}{N'} \rceil + 1}^{(u)}(b - N - (\lceil \frac{b-N}{N'} \rceil - 1)N') & \text{otherwise.} \end{cases} \quad (51)$$

The effective channel vector for transmitting signal $x_k^{(u)}(i)$ from UE k to BSs is

$$\tilde{\mathbf{f}}^{\text{UE } k \rightarrow \text{BSs}}(i) = \begin{cases} \tilde{\mathbf{f}}^{(u)}(:, i) & \text{if } k = 1, \\ \tilde{\mathbf{f}}^{(u)}(:, N + (k-2)N' + i) & \text{otherwise.} \end{cases} \quad (52)$$

Furthermore, the noise covariance at the BSs is also denoted by

$$(\sigma_{\tilde{f}^{(u)}(a,b)}^{(u)})^2 \mathbf{I}_N = (\sigma_{\lceil \frac{a}{N} \rceil}^{(u)})^2 \mathbf{I}_N. \quad (53)$$

The notations for the downlink can be defined likewise.

According to [19], the linear function of aligned interfering signals with noise can be decoded into an integer combination of the codewords rather than treating the interference as noise. In the SNC scheme, the effective channel coefficients in the aligned signals and the equation coefficients in the network-coded messages are exactly the same. Therefore, according to [19, Example 1], the achievable rate of transmitting signal $x_k^{(u)}(i)$ from UE k to BSs in the uplink can be further simplified to (48). The achievable rate of transmitting signal $x_l^{(d)}(i)$ from BS l to UEs in the downlink, $R_l^{(d)}(i)$, can be found likewise. ■

Second, we consider the achievable rate of the BS-CP link. As defined in the system model in Section II, the rate-constraint on conveying the message through the digital link is $R_0 = \log_2(1 + \bar{\rho})$, where $\bar{\rho}$ denotes the average SNR of the UE-BS links.

Finally, for the uplink, the end-to-end achievable rate of conveying the message $b_k^{(u)}(i)$ from UE k to the CP is

$$\tilde{R}_k^{(u)}(i) = \min\{R_k^{(u)}(i), R_0\}. \quad (54)$$

Therefore, the end-to-end sum-rates of the system for the uplink over an N symbol extension is

$$R_{\text{sum}}^{(u)} = \sum_k \sum_i \tilde{R}_k^{(u)}(i). \quad (55)$$

The rates for the downlink can be defined similarly.

Notice that N denotes the size of a supersymbol but not the length of the code. The rate is said to be achievable if there exists a code such that the probability of error can be arbitrary small as the block length tends to infinity. In this paper, we describe the SNC scheme in terms of one supersymbol. We focus on the designs of the precoding matrices for signal alignment and the network coding operations for mitigating the interference. As the nodes are not sending only one supersymbol during the whole transmission, we can concatenate supersymbols to adopt error correction schemes. The error control coding part is beyond the scope of this paper.

V. SIMULATION RESULTS

We present the simulation results to evaluate the finite SNR performance of the SNC scheme in both uplink and downlink time-varying C-RANs with rate-restricted digital links.

$$R_k^{(u)}(i) < \min_{\substack{\tilde{f}^{(u)}(a,b) \neq 0, \\ \tilde{\mathbf{f}}^{\text{UE } k \rightarrow \text{BSs}}(i)}} \log_2^+ \left(\frac{1}{\|\tilde{\mathbf{f}}^{(u)}(a, :)\|^2} + \frac{|\left(\mathbf{u}_{\tilde{f}^{(u)}(a,b)}^{(u)}\right)^H \left(\mathbf{H}_{\tilde{f}^{(u)}(a,b)}^{(u)}\right) \left(\mathbf{v}_{\tilde{f}^{(u)}(a,b)}^{(u)}\right)|^2}{\left(\mathbf{u}_{\tilde{f}^{(u)}(a,b)}^{(u)}\right)^H \left(\left(\sigma_{\tilde{f}^{(u)}(a,b)}^{(u)}\right)^2 \mathbf{I}_N \right) \left(\mathbf{u}_{\tilde{f}^{(u)}(a,b)}^{(u)}\right)} \right) \quad (48)$$

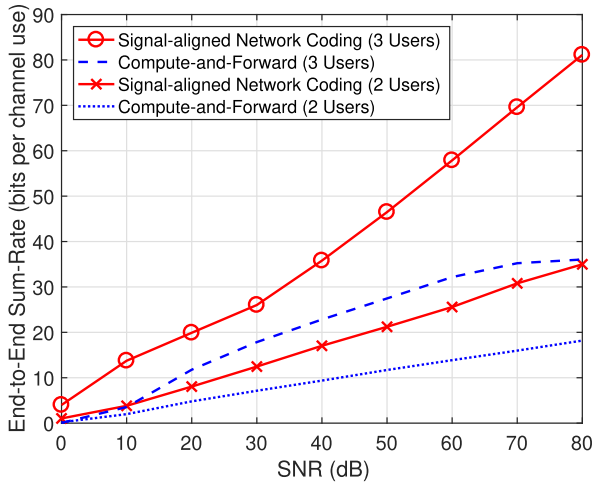


Fig. 3. Average end-to-end sum-rate achieved in uplink C-RAN.

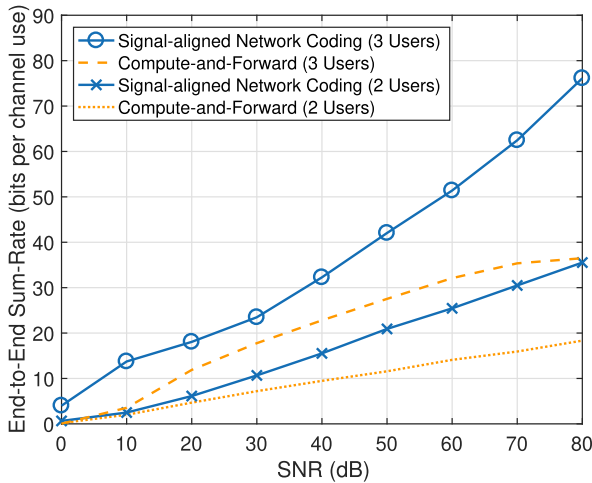


Fig. 4. Average end-to-end sum-rate achieved in downlink C-RAN.

We compare the end-to-end sum-rates of the SNC scheme with that of the conventional compute-and-forward scheme [19].

In the conventional compute-and-forward scheme, the selection of the optimal network coding coefficients in the linear combinations of messages over a finite field turns out to be a shortest vector problem (SVP) which is NP-hard. Therefore, we use the quantization algorithm presented in [43] to find the suboptimal network coding coefficients. This quantization algorithm considers the real-valued channel model; hence, we present the performances of all the schemes with real-valued channel coefficients in this section.

We assume that the transmit powers for each signal are the same, and the noise variances at each node are the same. We consider that all nodes are equipped with one antenna. We present the results of the two-user and the three-user cases with $n = 1$ and $q = 2$. The details of the symbol extension parameter n can be found at the beginning of Section IV.

We show the simulation results with respect to the ratio of the transmit power for each signal to the noise variance at each node (i.e., SNR value $\bar{\rho}$). We consider that the rate constraint on each digital link is $R_0 = \log_2(1 + \bar{\rho})$. The average end-to-end sum-rates are computed using 1000 random channel realizations. The obtained results for the uplink and the downlink are shown in Fig. 3 and 4 respectively.

Fig. 3 and 4 reveals that the SNC scheme achieves superior performance than the conventional compute-and-forward scheme for both the uplink and the downlink in the two-user and the three-user cases, especially in the high SNR regime. The sum-rate of the conventional compute-and-forward scheme is deteriorated by the rank deficiency and the non-integer penalty problems described in Section I. The performance improvement of the SNC scheme mainly comes from the proper designs of the network-coded messages transmitted and the alignment of signals.

VI. CONCLUSION

In this paper, we put forth the SNC scheme for both uplink and downlink multi-user time-varying MIMO C-RANs with rate-constrained digital links. Owing to the limited capacities of the digital links, joint processing of the raw signals directly cannot be applied to this channel model. The main idea of the SNC scheme is to strategically design the network-coded messages transmitted and the alignment of signals for mitigating the inter-cell interference. With a sufficiently large number of symbol extension, the users achieve arbitrarily close to full DoF as if there is unlimited cooperation between the BSs to perform joint processing. This achievement is not limited by the number of antennas of each node. Moreover, simulation results show that the finite SNR performance of the SNC scheme is better than the conventional compute-and-forward scheme.

APPENDIX A SNC FOR GENERAL MIMO CASES

In this section, we extend the SNC scheme to general cases. We consider that there are K UEs and L BSs, where K and L are not necessarily identical, in time-varying MIMO C-RAN with rate-constrained digital links. UE k has $M_k^{(UE)}$ antennas and BS l has $M_l^{(BS)}$ antennas.

For this channel model, we can simply consider each antenna of a node as a virtual node with an antenna. Loosely speaking, we consider that the rate constraints of the digital links for the virtual nodes and the capacities of the wireless links are of the same order of magnitude. The SNC scheme can be simply extended to the $L \neq K$ case by selecting a subset of the UEs or the BSs. In other words, the system activates both $M = \min\left(\sum_{k=1}^K M_k^{(UE)}, \sum_{l=1}^L M_l^{(BS)}\right)$ virtual UEs and virtual BSs. According to the result in Section IV, the users in this network achieve total $M = \min\left(\sum_{k=1}^K M_k^{(UE)}, \sum_{l=1}^L M_l^{(BS)}\right)$ DoF per slot asymptotically in both the uplink and the downlink cases.

APPENDIX B PROOF OF LEMMA 1

We first show that linear precoding matrix $\mathbf{V}_1^{(u)}$ has rank N . We prove $\det(\mathbf{V}_1^{(u)}) \neq 0$ almost surely by contradiction. We denote the (i, j) entry of linear precoding matrix $\mathbf{V}_1^{(u)}$ by $v_1^{(i,j)(u)}$ where $i \in \{1, 2, \dots, N\}$ and $j \in \{1, 2, \dots, N\}$.

We also denote the (i, j) cofactor of $\mathbf{V}_1^{(u)}$ by $A_1^{(i,j)(u)}$. We expand $\det(\mathbf{V}_1^{(u)})$ along the first row, i.e.,

$$\det(\mathbf{V}_1^{(u)}) = v_1^{(1,1)(u)} A_1^{(1,1)(u)} + v_1^{(1,2)(u)} A_1^{(1,2)(u)} + \cdots + v_1^{(1,N)(u)} A_1^{(1,N)(u)}. \quad (56)$$

Notice that none of cofactor $A_1^{(1,j)(u)}$ depends on $v_1^{(1,1)(u)}$. If all values of cofactor $A_1^{(1,j)(u)}$ and entry $v_1^{(1,j)(u)}$ except entry $v_1^{(1,1)(u)}$ are known, (56) is a polynomial equation in $v_1^{(1,1)(u)}$. $\det(\mathbf{V}_1^{(u)}) = 0$ implies two possibilities:

- 1) $v_1^{(1,1)(u)}$ is the root of the equation.
- 2) $A_1^{(1,1)(u)} = 0$ and $v_1^{(1,2)(u)} A_1^{(1,2)(u)} + v_1^{(1,3)(u)} A_1^{(1,3)(u)} + \cdots + v_1^{(1,N)(u)} A_1^{(1,N)(u)} = 0$.

As entry $v_1^{(1,1)(u)}$ is the multiplication of channel coefficients which are drawn from a continuous distribution, case 1 is impossible almost surely.

Then we focus on the case that the $(1, 1)$ cofactor $A_1^{(1,1)(u)} = 0$. Cofactor $A_1^{(1,1)(u)}$ can be regarded as the determinant of the submatrix formed by eliminating the first row and the first column of $\mathbf{V}_1^{(u)}$. Afterward, we keep deducing the determinant of the submatrix formed by eliminating the first row and the first column of the matrix is required to be zero repeatedly. Finally, we obtain the deduction that $v_1^{(N,N)(u)} = 0$. However, it is almost impossible because all entries $v_1^{(i,j)(u)}$ are drawn from a continuous distribution randomly. Hence, $\det(\mathbf{V}_1^{(u)}) \neq 0$ is proved by contradiction, and linear precoding matrix \mathbf{V}_1 has rank N almost surely.

As the matrix formed by the first N' rows of $\mathbf{V}_{k'}^{(u)}$, $k' \in \{2, 3, \dots, K\}$, has a similar structure to $\mathbf{V}_1^{(u)}$, $\mathbf{V}_{k'}^{(u)}$ can be proved to have rank N' likewise. This proof is omitted to avoid repetition.

APPENDIX C PROOF OF LEMMA 2

We first assume binary matrix $\mathbf{F}^{(u)}$ is in the field of complex numbers and decompose it into matrix multiplications $[(\mathbf{U}^{(u)})^H] [\mathbf{H}^{(u)}] [\mathbf{V}^{(u)}]$ where

$$[(\mathbf{U}^{(u)})^H] = \text{diag} \left[(\mathbf{U}_1^{(u)})^H \quad (\mathbf{U}_2^{(u)})^H \quad \cdots \quad (\mathbf{U}_L^{(u)})^H \right], \quad (57)$$

$$[\mathbf{H}^{(u)}] = \begin{bmatrix} \mathbf{H}_{1,1}^{(u)} & \mathbf{H}_{1,2}^{(u)} & \cdots & \mathbf{H}_{1,K}^{(u)} \\ \mathbf{H}_{2,1}^{(u)} & \mathbf{H}_{2,2}^{(u)} & \cdots & \mathbf{H}_{2,K}^{(u)} \\ \vdots & \vdots & \ddots & \vdots \\ \mathbf{H}_{L,1}^{(u)} & \mathbf{H}_{L,2}^{(u)} & \cdots & \mathbf{H}_{L,K}^{(u)} \end{bmatrix}, \quad \text{and} \quad (58)$$

$$[\mathbf{V}^{(u)}] = \text{diag} \left[\mathbf{V}_1^{(u)} \quad \mathbf{V}_2^{(u)} \quad \cdots \quad \mathbf{V}_K^{(u)} \right]. \quad (59)$$

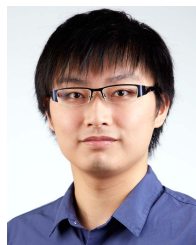
As mentioned in Section IV, $N \times N$ matrices $(\mathbf{U}_i^{(u)})^H$ and $\mathbf{V}_1^{(u)}$ have rank N . Moreover, $N \times N'$ matrix $\mathbf{V}_{k'}^{(u)}$, $k' \in \{2, 3, \dots, K\}$, has rank N' . Recall that all channel coefficients in $N \times N$ matrix $\mathbf{H}_{i,k}^{(u)}$ are drawn from a continuous distribution randomly. Therefore, $\mathbf{F}^{(u)}$ has rank $N + (K - 1)N'$. We can pick any $N + (K - 1)N'$ independent rows of $\mathbf{F}^{(u)}$ to form an $(N + (K - 1)N') \times (N + (K - 1)N')$ invertible binary matrix $\mathbf{F}'^{(u)}$, which means $\det(\mathbf{F}'^{(u)}) \neq 0$. There must exist some q such that $\det(\mathbf{F}'^{(u)}) \bmod q \neq 0$; hence binary

matrix $\mathbf{F}^{(u)}$ has rank $N + (K - 1)N'$ for some finite field sizes q .

REFERENCES

- [1] T.-T. Chan and T.-M. Lok, "Signal-aligned network coding in interference channels with limited receiver cooperation," in *Proc. IEEE/CIC Int. Conf. Commun. China (ICCC)*, Aug. 2018, pp. 573–577.
- [2] T.-T. Chan and T.-M. Lok, "Reverse signal-aligned network coding in interference channels with limited transmitter cooperation," in *Proc. IEEE Int. Conf. Signal Process., Commun. Comput. (ICSPCC)*, Sep. 2018, pp. 1–6.
- [3] D. Gesbert, S. Hanly, H. Huang, S. Shamai (Shitz), O. Simeone, and W. Yu, "Multi-cell MIMO cooperative networks: A new look at interference," *IEEE J. Sel. Areas Commun.*, vol. 28, no. 9, pp. 1380–1408, Dec. 2010.
- [4] O. Simeone, A. Maeder, M. Peng, O. Sahin, and W. Yu, "Cloud radio access network: Virtualizing wireless access for dense heterogeneous systems," *J. Commun. Netw.*, vol. 18, no. 2, pp. 135–149, Apr. 2016.
- [5] M. Peng, C. Wang, V. Lau, and H. V. Poor, "Fronthaul-constrained cloud radio access networks: Insights and challenges," *IEEE Wireless Commun.*, vol. 22, no. 2, pp. 152–160, Apr. 2015.
- [6] S. Zhang, S. C. Liew, and P. P. Lam, "Hot topic: Physical-layer network coding," in *Proc. ACM MobiCom*, 2006, pp. 358–365.
- [7] R. Ahlswede, N. Cai, S.-Y. R. Li, and R. W. Yeung, "Network information flow," *IEEE Trans. Inf. Theory*, vol. 46, no. 4, pp. 1204–1216, Jul. 2000.
- [8] S.-Y. R. Li, R. W. Yeung, and N. Cai, "Linear network coding," *IEEE Trans. Inf. Theory*, vol. 49, no. 2, pp. 371–381, Feb. 2003.
- [9] T. Peng, Y. Wang, A. G. Burr, and M. R. Shikh-Bahaei, "Physical layer network coding in network MIMO: A new design for 5G and beyond," *IEEE Trans. Commun.*, vol. 67, no. 3, pp. 2024–2035, Mar. 2019.
- [10] O. Simeone, O. Somekh, H. V. Poor, and S. Shamai (Shitz), "Downlink multicell processing with limited-backhaul capacity," *EURASIP J. Adv. Signal Process.*, vol. 2009, no. 3, pp. 1–10, Feb. 2009.
- [11] A. Sanderovich, O. Somekh, H. V. Poor, and S. Shamai (Shitz), "Uplink macro diversity of limited backhaul cellular network," *IEEE Trans. Inf. Theory*, vol. 55, no. 8, pp. 3457–3478, Aug. 2009.
- [12] S.-H. Park, O. Simeone, O. Sahin, and S. Shamai (Shitz), "Joint decompression and decoding for cloud radio access networks," *IEEE Signal Process. Lett.*, vol. 20, no. 5, pp. 503–506, May 2013.
- [13] L. Zhou and W. Yu, "Uplink multicell processing with limited backhaul via per-base-station successive interference cancellation," *IEEE J. Sel. Areas Commun.*, vol. 31, no. 10, pp. 1981–1993, Oct. 2013.
- [14] S.-H. Park, O. Simeone, O. Sahin, and S. Shamai (Shitz), "Joint precoding and multivariate backhaul compression for the downlink of cloud radio access networks," *IEEE Trans. Signal Process.*, vol. 61, no. 22, pp. 5646–5658, Nov. 2013.
- [15] P. Patil and W. Yu, "Hybrid compression and message-sharing strategy for the downlink cloud radio-access network," in *Proc. Inf. Theory Appl. Workshop (ITA)*, Feb. 2014, pp. 1–6.
- [16] Y. Zhou and W. Yu, "Optimized backhaul compression for uplink cloud radio access network," *IEEE J. Sel. Areas Commun.*, vol. 32, no. 6, pp. 1295–1307, Jun. 2014.
- [17] Y. Zhou and W. Yu, "Fronthaul compression and transmit beamforming optimization for multi-antenna uplink C-RAN," *IEEE Trans. Signal Process.*, vol. 64, no. 16, pp. 4138–4151, Aug. 2016.
- [18] B. Nazer, A. Sanderovich, M. Gastpar, and S. Shamai (Shitz), "Structured superposition for backhaul constrained cellular uplink," in *Proc. IEEE Int. Symp. Inf. Theory*, Jun. 2009, pp. 1530–1534.
- [19] B. Nazer and M. Gastpar, "Compute-and-forward: Harnessing interference through structured codes," *IEEE Trans. Inf. Theory*, vol. 57, no. 10, pp. 6463–6486, Oct. 2011.
- [20] L. Wei and W. Chen, "Compute-and-forward network coding design over multi-source multi-relay channels," *IEEE Trans. Wireless Commun.*, vol. 11, no. 9, pp. 3348–3357, Sep. 2012.
- [21] H. Najafi, M. O. Damen, and A. Hjørungnes, "Asynchronous compute-and-forward," *IEEE Trans. Commun.*, vol. 61, no. 7, pp. 2704–2712, Jul. 2013.
- [22] S.-N. Hong and G. Caire, "Compute-and-forward strategies for cooperative distributed antenna systems," *IEEE Trans. Inf. Theory*, vol. 59, no. 9, pp. 5227–5243, Sep. 2013.
- [23] M. El Soussi, A. Zaidi, and L. Vandendorpe, "Compute-and-forward on a multi-user multi-relay channel," *IEEE Wireless Commun. Lett.*, vol. 3, no. 6, pp. 589–592, Dec. 2014.

- [24] T. Yang, Q. T. Sun, J. A. Zhang, and J. Yuan, "A linear network coding approach for uplink distributed MIMO systems: Protocol and outage behavior," *IEEE J. Sel. Areas Commun.*, vol. 33, no. 2, pp. 250–263, Feb. 2015.
- [25] Z. Chen, P. Fan, and K. B. Letaief, "Compute-and-forward: Optimization over multisource–multirelay networks," *IEEE Trans. Veh. Technol.*, vol. 64, no. 5, pp. 1806–1818, May 2015.
- [26] T. Yang, X. Yuan, and Q. T. Sun, "A signal-space aligned network coding approach to distributed MIMO," *IEEE Trans. Signal Process.*, vol. 65, no. 1, pp. 27–40, Jan. 2017.
- [27] T. Yang, "Distributed MIMO broadcasting: Reverse compute-and-forward and signal-space alignment," *IEEE Trans. Wireless Commun.*, vol. 16, no. 1, pp. 581–593, Jan. 2017.
- [28] H. Cheng, X. Yuan, and T. Yang, "Generalized signal-space alignment based physical-layer network coding for distributed MIMO systems," *IEEE Access*, vol. 7, pp. 48430–48444, 2019.
- [29] T. Gou, S. A. Jafar, S.-W. Jeon, and S.-Y. Chung, "Aligned interference neutralization and the degrees of freedom of the $2 \times 2 \times 2$ interference channel," in *Proc. IEEE Int. Symp. Inf. Theory*, Jul. 2011, pp. 2751–2755.
- [30] I. Shomorony and A. S. Avestimehr, "Degrees of freedom of two-hop wireless networks: Everyone gets the entire cake," *IEEE Trans. Inf. Theory*, vol. 60, no. 5, pp. 2417–2431, May 2014.
- [31] S. A. Jafar and S. Shamai (Shitz), "Degrees of freedom region of the MIMO X channel," *IEEE Trans. Inf. Theory*, vol. 54, no. 1, pp. 151–170, Jan. 2008.
- [32] M. A. Maddah-Ali, A. S. Motahari, and A. K. Khandani, "Communication over MIMO X channels: Interference alignment, decomposition, and performance analysis," *IEEE Trans. Inf. Theory*, vol. 54, no. 8, pp. 3457–3470, Aug. 2008.
- [33] V. R. Cadambe and S. A. Jafar, "Interference alignment and degrees of freedom of the K-user interference channel," *IEEE Trans. Inf. Theory*, vol. 54, no. 8, pp. 3425–3441, Aug. 2008.
- [34] R. Tandon and O. Simeone, "Cloud-aided wireless networks with edge caching: Fundamental latency trade-offs in fog radio access networks," in *Proc. IEEE Int. Symp. Inf. Theory (ISIT)*, Jul. 2016, pp. 2029–2033.
- [35] A. Sengupta, R. Tandon, and O. Simeone, "Fog-aided wireless networks for content delivery: Fundamental latency tradeoffs," *IEEE Trans. Inf. Theory*, vol. 63, no. 10, pp. 6650–6678, Oct. 2017.
- [36] N. Lee, J.-B. Lim, and J. Chun, "Degrees of freedom of the MIMO Y channel: Signal space alignment for network coding," *IEEE Trans. Inf. Theory*, vol. 56, no. 7, pp. 3332–3342, Jul. 2010.
- [37] R. Zhou, Z. Li, C. Wu, and C. Williamson, "Signal alignment: Enabling physical layer network coding for MIMO networking," *IEEE Trans. Wireless Commun.*, vol. 12, no. 6, pp. 3012–3023, Jun. 2013.
- [38] Y. Tian and A. Yener, "Degrees of freedom for the MIMO multi-way relay channel," *IEEE Trans. Inf. Theory*, vol. 60, no. 5, pp. 2495–2511, May 2014.
- [39] H. Mu and J. K. Tugnait, "Achievable degrees of freedom for K-user MIMO Y channels using signal group based alignment," *IEEE Trans. Wireless Commun.*, vol. 13, no. 8, pp. 4520–4533, Aug. 2014.
- [40] X. Yuan, "MIMO multiway relaying with clustered full data exchange: Signal space alignment and degrees of freedom," *IEEE Trans. Wireless Commun.*, vol. 13, no. 12, pp. 6795–6808, Dec. 2014.
- [41] K. Liu and M. Tao, "Generalized signal alignment: On the achievable DoF for multi-user MIMO two-way relay channels," *IEEE Trans. Inf. Theory*, vol. 61, no. 6, pp. 3365–3386, Jun. 2015.
- [42] T.-T. Chan and T.-M. Lok, "Interference alignment with physical-layer network coding in MIMO relay channels," in *Proc. IEEE Int. Conf. Commun. (ICC)*, May 2016, pp. 1–6.
- [43] B. Zhou and W. H. Mow, "A quadratic programming relaxation approach to compute-and-forward network coding design," in *Proc. IEEE Int. Symp. Inf. Theory*, Jun. 2014, pp. 2296–2300.



Tse-Tin Chan (Student Member, IEEE) received the B.Eng. degree in information engineering from The Chinese University of Hong Kong, Hong Kong, in 2014, where he is currently pursuing the Ph.D. degree in information engineering.

He is currently working on the researches about interference alignment and physical-layer network coding. His research interests are in wireless communications and machine learning.



Tat-Ming Lok (Senior Member, IEEE) received the B.Sc. degree in electronic engineering from The Chinese University of Hong Kong and the M.S.E.E. degree and the Ph.D. degree in electrical engineering from Purdue University.

He was a Postdoctoral Research Associate with Purdue University. He then joined The Chinese University of Hong Kong, where he is currently an Associate Professor. His research interests include communication theory, communication networks, signal processing for communications, and wireless systems. He has served on TPCs for many international conferences, including IEEE ICC, VTC, GLOBECOM, WCNC, ISIT, and so on. He has also served on the editorial boards for several international journals, including IEEE TRANSACTIONS ON VEHICULAR TECHNOLOGY from 2002 to 2008 and IEEE TRANSACTIONS ON WIRELESS COMMUNICATIONS from 2015 to 2018.